

# Evaluation of a latent heat thermal energy storage system using AlSi12 as a phase change material

Johannes P. Kotzé

Stellenbosch University

Centre for Renewable and Sustainable Energy Studies

## Abstract

Latent heat thermal energy storage in metallic phase-change materials may allow thermal energy storage at temperatures far higher than currently possible with any sensible thermal energy storage system. Kotzé, Von Backström & Erens proposes a concept for a thermal energy storage unit that can utilise metallic phase-change materials and metallic heat transfer fluids in a safe manner. Using their concept, a model was created using the simulation software Flownex to evaluate Kotzé *et al.*'s theory. The model incorporates all heat-transfer, storage and power-generating equipment in as much detail as possible. It also enables the evaluation of every aspect of the plant; and can be used to study the effects of various design variables on the overall plant performance. It was used to calculate a feasible plant design for a CSP plant that can deliver 100MWe base load power in Upington, South Africa.

Key words: Metallic PCM, NaK, Heat transfer, Thermal energy storage, CSP

## 1. Introduction

A thermal energy storage system using metallic phase-change materials (PCM) was proposed by Kotzé, Von Backström & Erens [1]. Among the prospective PCMs, AlSi12 was identified as a viable storage material for high temperature, thermal energy storage.

AlSi12 is commonly available and has a relatively moderate melting point of 577°C. Theory established with it can then be used for higher melting temperature PCMs such as eutectic MgSi (946°C) [2].

To utilise these high melting point, metallic PCMs, a high temperature heat transfer fluid (HTF) is needed. The use of liquid sodium-potassium alloy (NaK) has been proposed[3], but a major concern when using it as a HTF is that it is highly reactive with water. While NaK-water heat exchangers are common in the nuclear industry [4], it is still regarded with considerable caution in the solar industry.

These factors have led to an innovative design by Kotzé *et al.* for a combined thermal energy storage- and steam generator unit [1]. The inherently high thermal conductivity of metallic PCMs can be used to build a thermal storage unit and steam generator that physically separates NaK from the water by using the metallic PCM as a buffer. While the thermodynamic viability of the system is easily proven, there are some practical challenges that need to be considered to prove the viability of the system, including:

- heat transfer modes;
- design parameters;
- process control; and
- long-term stability of the PCM.

To evaluate the first three considerations, an accurate simulation or model of the entire power cycle, storage and receiver system is required. The model, constructed using Flownex SE, will also serve as a design tool for such a system. The operation of this model is the topic of this paper

The model, depicted in Figure 1 below, consists of a number of smaller models that is discussed in the paper. The heat-transfer models and power cycle simulation are all conducted in the network solver; whereas the storage- and the solar input model is a time-dependent mathematical model.

The model can be used for a cost analysis and in both steady-state and transient analyses. This permits the evaluation of the effects of a vast array of variables, including operational conditions and design parameters. The long-term stability of the storage material and validity of the assumptions made in the Flownex model is being validated with a physical experiment that is still in progress.

For analysis a hypothetical solar power plant is modelled that can deliver 100MW base load power throughout the year. The town Upington, in the Northern Cape province of South Africa, was chosen as the location for this hypothetical power plant.

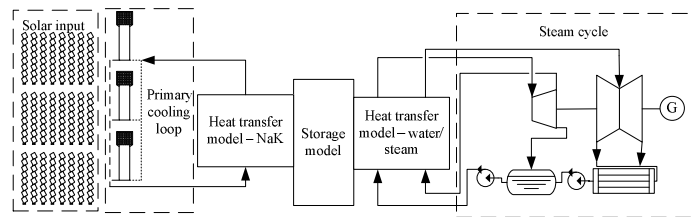


**Fig.1. Overview of the Flownex model**

In this paper the heat of fusion ( $H_f$ ) of AlSi12 is assumed to be 548.6J/g; and the melting point to be 577°C [1].

## 2. Steam cycle

To be able to design and analyse the heat transfer surfaces in the storage unit, it was necessary to model both the primary heat-transfer loop (NaK) and the steam power cycle in as much detail as possible. The model that was constructed is depicted in Figure 2 below; the specifications being:

- 100MW electrical output;
- 540°C, 140 bar superheat;
- 540°C, 30 bar re-heat;
- one openfeed water heater supplied from the high-pressure turbine outlet; and
- an air-cooled condenser.

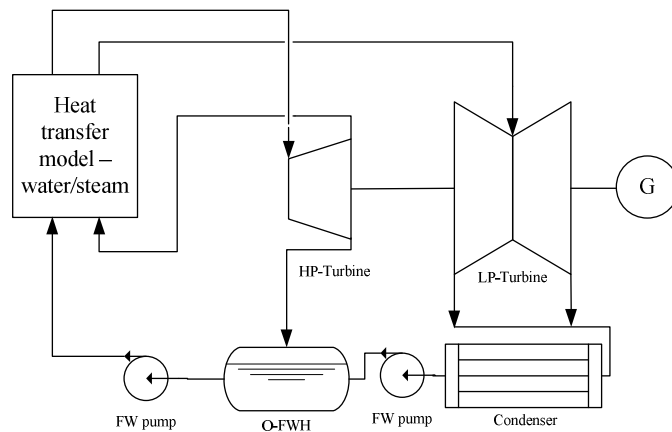


**Fig.2. - Power plant model**

The pumps and the turbines were modelled using generic turbine and pump charts that are built into Flownex, of which the design efficiency is indicated in Table 1. Table 1 is a summary of the energy balance of the steam cycle. Notably the cycle's overall thermal efficiency is calculated to be 43% between the thermal input from storage and the electrical output of the system (the heat source is at 577°C and sink is 25°C). This is slightly higher than the 40.7% predicted by the Chambadal-Novikov efficiency correlation [5]. It must be noted that the simulation do not incorporate all the power plant components and that the efficiencies of the components are not a true reputation of actual hardware.

<b>Thermal input:</b>			Efficiency
Boiler	131.50	MW	
Super-heater	69.32	MW	
Re-heater	35.87	MW	
<b>Total</b>	<b>236.69</b>	<b>MW</b>	
<b>Turbine mechanical output:</b>			
High pressure turbine	35.03	MW	0.95
Low pressure turbine	73.40	MW	0.95
<b>Total</b>	<b>108.43</b>	<b>MW</b>	
<b>Generator Electrical output</b>	<b>103.01</b>	<b>MW</b>	0.95
<b>Pump electrical input:</b>			
Feedwater pump 1	240.65	kW	0.90
Feedwater pump 2	19.10	kW	0.90
Boiler pump	17.07	kW	0.90
NaK pump (peak)	559.04	kW	0.90
Condenser pump	26.73	kW	0.90
<b>Total</b>	<b>862.59</b>	<b>kW</b>	
<b>Nett electrical output</b>	<b>102.15</b>	<b>MW</b>	0.43

**Table 1 - Energy balance of the power cycle**

Table 2 below shows the boundary conditions that were obtained using the model and that were applied for the design of the heat transfer surfaces in the steam generator. The steam generator is divided into three sections, namely boiler, super-heater and re-heater. Each of these sections is contained in separate storage units. The heat-transfer pipes for both the NaK side and the steam side are embedded into the PCM. All the heat-transfer pipes are evenly spaced.

Legend: SCL - Sub-cooled Liquid SatS - Saturated steam SHS - Super-heated steam	Inlet temperature	Inlet pressure	State/ Inlet Quality	Outlet temperature	Outlet pressure	State/ Outlet Quality	Mass flow
	°C	Bar	x	°C	Bar	x	kg/s
<b>Boiler</b>	237.0	145.0	SCL	339.4	145.0	SatS	86.1
<b>Super-heater</b>	339.2	144.5	1	540.0	144.2	SHS	86.1
<b>Re-heater</b>	32.9	314.7	SHS	540.0	32.5	SHS	68.7

**Table 2 - Boundary conditions yielded by the steam cycle model**

### 3. Storage model

The storage model monitors the energy stored in the phase-change material, and returns storage conditions to the heat transfer models (discussed in sections 4 and 5 below). The working of this model is described in Figure 3 below.

In the model two assumptions are made: It is assumed that the PCM solidifies in a cylinder around the heat transfer pipes. Secondly it is assumed that the NaK heat transfer pipes and steam heat transfer pipes do not interfere with each other. This assumption is made for simplification, but is rationalised by the fact that the majority of the discharge cycle occurs if there is no thermal input from the NaK system.

The storage model is implemented using an Excel spread sheet incorporated into the Flownex model. The model monitors the charge state, denoted as "x", of each of the storage units. If all the PCM is molten, x=1; and when all the PCM has solidified, x=0. The model monitors the thermal energy added to or removed from the storage unit using the following equation:

$$E_{Store} = E_{in} - E_{out} = \int_0^t Q_{in} \cdot dt - \int_0^t Q_{out} \cdot dt$$

In the equation,  $Q_{in}$  and  $Q_{out}$  are determined by the heat transfer models. The initial state of the model needs to be fixed manually, and should be established according to the required analysis. The charge state is calculated by:

$$x_m = \frac{E_{stored}}{E_{total}} = \frac{E_{stored}}{m \cdot H_f}$$

In the equation,  $m$  is the total mass of PCM and  $H_f$  is the heat of fusion of the PCM.

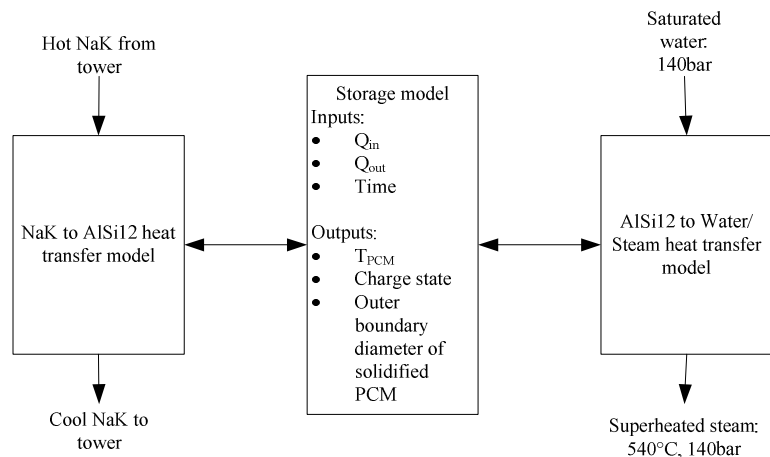


**Fig.3. - Thermal storage model**

The temperature of the PCM ( $T_{PCM}$ ) can move into the sensible heat regions above and below the melting point if the charge falls above or below the latent heat region. If the PCM is in the latent heat mode and in the process of melting or thawing, the model passes the melting point of the PCM through to the heat transfer models. If the PCM moves into the sensible region,  $T_{PCM}$  is calculated using the specific heat capacity of the PCM.

The heat transfer pipes of the heat exchangers are spaced evenly throughout the PCM. For each heat transfer pipe in the steam generator, there is therefore an “area” of PCM that “services” that pipe. Ignoring the outer edges of the storage tank, the cross-section of the tank can be divided into hexagons. As the solidified PCM grows out around the heat transfer pipes, these cylinders of solidified PCM will grow towards each other until they touch.

The cylinders will start to interfere at the maximum outer boundary diameter ( $d_{MOB}$ ). The outer boundary diameter ( $d_{OB}$ ) of these cylinders is calculated based on the charge state of the PCM. The outer boundary diameter is passed through to the heat transfer model in the steam side to calculate the thermal resistance of the solidified PCM.

In Figure 4 below it is seen that after the outer boundary diameter reaches  $d_{MOB}$ , there will be some interference of the solidified cylinders. This causes the area exposed to molten PCM to rapidly decrease as the storage unit discharges. It can be geometrically proven that if the cylinders expand to the point where they touch each other, the charge state ( $x$ ) of the system is 0.093.

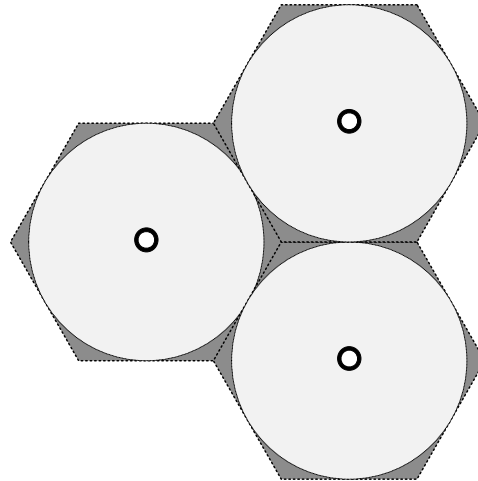


**Fig.4. - Illustration of PCM solidification when solidified cylinders start to interfere**

The size of the storage system is determined by the number of hours of storage that the system should run from storage. Using the Bird clear sky model, it was determined that to ensure base load operation of the plant, 15h of storage is needed (refer to section 5 below). If the storage unit is designed to operate completely in the latent heat mode, the required mass of PCM is calculated through the equation:

$$m_{pcm} = 1.093(\dot{Q}_{th} \cdot t \cdot H_f)$$

Where  $\dot{Q}_{th}$  is the required thermal output of the storage unit;  $t$  is the required storage time; and  $H_f$  is the heat of fusion of the PCM. The amount 1.093 is used to account for the PCM in the spaces between the cylinders (Figure 4). In Table 3 the sizing of the storage tanks is presented.

	Boiler	Super-heater	Re-heater
Number of tanks	10	8	2
Tank diameter	10.80 m	9.60 m	6.50 m
Tank height	6 m	5 m	10 m
Steam pipes per tank	30	102	250
NaK pipes per tank	100	100	200
Total mass of AlSi12	12943 ton	6625 ton	2648 ton
Total volume of AlSi12	4884 m <sup>3</sup>	2500 m <sup>3</sup>	1000 m <sup>3</sup>

**Table 3 - Storage tanks**

#### **4. Heat transfer model: Steam/water**

The basic variables of the heat exchangers in the steam generator sections include the length of the heat-transfer pipes; the number of tubes; and the tube size. A discretised model of these heat transfer surfaces is implemented in Flownex; and the model is then used to obtain the sizing of the heat transfer surfaces.

The Flownex heat transfer model can be best described through a resistance diagramme as the heat transfer model is based on nodes. It is possible to set up a heat transfer problem and to further increase its accuracy through discretisation (along both the length and the thickness of the heat transfer element). It was furthermore possible to determine the minimum number of required increments that would make no more than 0.1%

variation in the total calculated heat transfer by performing a sensitivity analysis. Material and fluid properties are evaluated using an extensive properties database.

Figure 5 below shows a section through one of the heat transfer pipes, with geometry annotations that will be used throughout the discussion. The thermal resistance network diagram is depicted beside it. The outer boundary diameter ( $d_{OB}$ ) in the figure denotes the diameter of the solidified PCM around the steam pipe; and  $d_{MOB}$  signifies the maximum outer boundary diameter. The spacing of the heat-transfer pipes limits  $d_{MOB}$ . The inside and outside diameters of the heat-transfer pipes are  $d_i$  and  $d_o$  respectively. This model is generic for the all three steam generator sections.

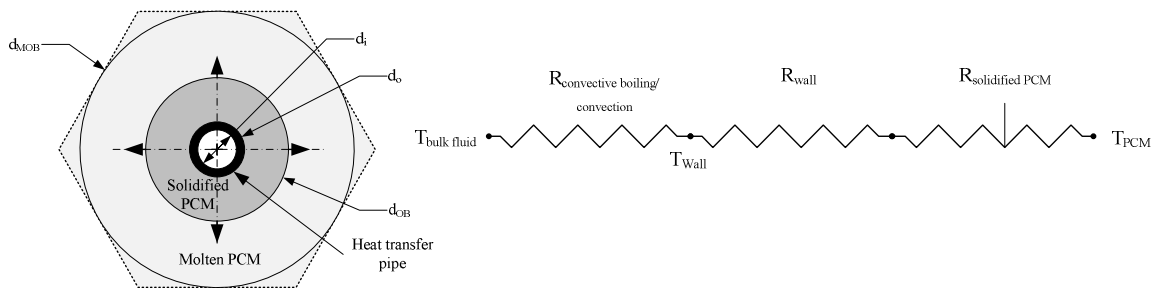


**Fig.5. - Section through one stem pipe showing annotation for analysis**

The convective boiling and -resistances depend on which part of the steam generator is analysed. In the re-heater and super-heater, the heat-transfer mechanism is purely convective; in which case the Gnielinski [6] equation is used to calculate the Nusselt number.

In the boiler, the heat-transfer mechanism is convective or flow boiling and a two-phase flow problem. Two-phase flow and heat transfer is exceptionally difficult to calculate and predict accurately, but there are various ways to consider a two-phase flow problem.

One approach is to deal with the two-phase fluid as a homogeneous mixture - a model that is suitable for the heat transfer problem in question. Flow boiling occurs in various regions and there are diverse boiling regimes; each with a different heat transfer correlation. The onset of nucleate boiling, saturated boiling and Leidenfrost points are calculated automatically in Flownex. The heat transfer coefficient is calculated using the Steiner and Taborek [7] correlation. In transition boiling, a linear extrapolation between the critical heat flux and the minimum heat flux points is used [8]; and for film boiling the Zuber correlation is used[8].

On the PCM side of the heat transfer surfaces (the heat transfer pipes is embedded into the PCM), there is a moving boundary problem. As the storage system discharges, solidified PCM builds up around the heat transfer pipes, causing a variation in the heat transfer characteristics of the heat exchange surfaces.

The diameter of this PCM build-up ( $d_{OB}$ ) is modelled in the storage model and is sent to the heat transfer model. For the plant to operate at steady conditions, the effect of the moving boundary needs to be counteracted. There is nothing that can be explicitly controlled about the energy source to the heat transfer surfaces (as in a gas-fired boiler), and the only feasible method of control is to manage the flow in the heat exchangers.

Flow boiling is a function of both convective boiling heat transfer and nucleate boiling heat transfer [9]. To therefore have a controllable steam generator, the convective/ convective-boiling h-at transfer should be the controlling heat transfer mechanism in the heat exchanger, especially close to complete discharge (as  $d_{OB}$  approaches  $d_{MOB}$ )

#### 4.1. Design and heat transfer control

Because the super-heater and re-heater operates on single phase it is possible to bypass some of the steam past the re-heater or super heater, and mix it with the superheated steam that went through the heat transfer pipes. This arrangement is shown in Figure 6. The heat exchangers for both the super-heater and re-heater were designed to deliver superheated steam with all of the steam running through the heat exchanger at the end of its charge. Thus, at higher charge states more steam will be diverted past the heat exchangers. The effectiveness of this control strategy has been tested using the model, and is further discussed in section 6

For the multiphase heat exchanger (boiler) the objective is to deliver saturated dry steam at the feedwater flow rate. Heat transfer gets impeded, and prediction methods are less accurate as soon as the liquid water separates from the heat transfer surface and forms a sustained vapour layer. This point is known as the Leidenfrost point. For this reason the heat exchange surfaces were designed so that there is no Leidenfrost point along the length of the heat transfer surfaces. This is done by keeping the vapour fraction sufficiently low in the boiler itself, and this means that the flow rate through the boiler should be multiple times that of the feedwater. The process layout is shown in Figure 6.

The first design point is done assuming the charge state of  $x=1$ . The design was not optimised, but a working design point was found using the Flownex designer and optimiser. The second design point was done for a charge state of 0.093. The same heat exchanger geometry was found for the first design point and the flow rate was increased to a point where the heat transfer rate was the same as that in the first design point. The design was manually iterated until the pressure drop variation over the heat exchanger was within acceptable limits. Using the boundary conditions in Table 2, the heat exchanger geometry presented in Table 4 was calculated.

<i>Steam/water heat exchange surfaces</i>			
	Boiler	Super-heater	Re-heater
Number of steam pipes	300	410	500
Diameter of steam pipes	33.40 mm	33.40 mm	33.40 mm
Wall thickness	4.55 mm	4.55 mm	4.55 mm
Length	6 m	10 m	10 m
Material	MS	MS	MS
<i>NaK heat transfer surfaces</i>			
	Boiler	Super-heater	Re-heater
Number of steam pipes	1000	800	400
Diameter of steam pipes	33.40 mm	33.40 mm	33.40 mm
Wall thickness	4.55 mm	4.55 mm	4.55 mm
Length	6 m	5 m	10 m
Material	SS	SS	SS

**Table 4 - Geometry of the heat exchangers**



		Full charge		Low charge	
Boiler	Boiler circulation rate	175.00	kg/s	400.00	kg/s
	Heat transfer	131.5	MW	131.5	MW
	Average convective boiling heat transfer coefficient	7759.21	W/m <sup>2</sup> .K	21301.32	W/m <sup>2</sup> .K
	d <sub>OB</sub>	0	m	1.85	m
Super-heater	Super-heater bypass	2.77	%	0.33	%
	Heat transfer	69.32	MW	69.32	MW
	Average convective heat transfer coefficient	2459.23	W/m <sup>2</sup> .K	2557.21	W/m <sup>2</sup> .K
	d <sub>OB</sub>	0	m	0.89	m
Re-heater	Re-heater bypass	9.01	%	8.22	%
	Heat transfer	35.87	MW	35.87	MW
	Average convective heat transfer coefficient	1239.27	W/m <sup>2</sup> .K	1246.03	W/m <sup>2</sup> .K
	d <sub>OB</sub>	0	m	0.58	m

**Table 5 - Steam generator operational parameters**

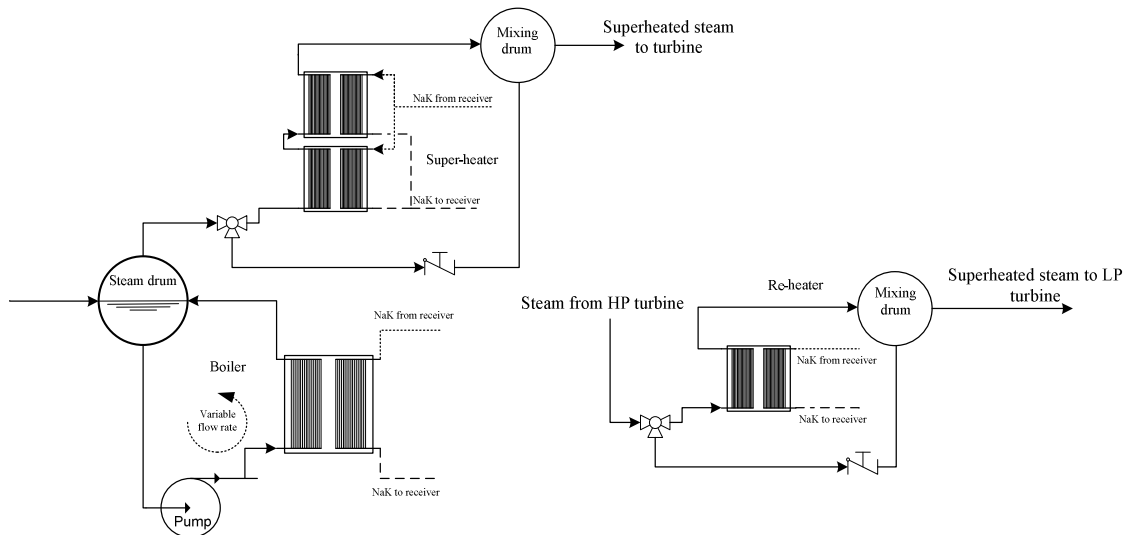


**Fig.6. - Schematic of steam generating equipment**

### 5. Heat transfer model: NaK

The isothermal nature of the storage unit decouples the heat transfer of the steam heat exchangers from that of the NaK heat exchangers; allowing the the NaK loop to be considered separately. The modelled thermal input is based on the Bird clear sky model [10] for a winter's day in Upington.

The time-dependent thermal input of the model is based on the normalised DNI output of the Bird clear sky model. This is shown in Figure 7, where the normalised DNI for both winter and summer are depicted by solid lines. As the hypothetical plant is required to operate at base load throughout the year, the system will be designed to cope with a winter scenario.

The required thermal energy that needs to be collected and transferred into the storage system is the product of the constant thermal output of the steam generator and 24h. By integrating the normalised DNI, it is possible to determine how much the normalised DNI needs to be scaled to yield a solar input profile that will deliver enough thermal energy to the storage units to operate the entire plant.

The thermal input profiles of both winter and summer is denoted with the dotted lines in Figure 7 and is read on the secondary axis on the right. Using the winter thermal input profile it is also possible to determine the peak heat transfer conditions that are required from the primary cooling loop. The heat transfer requirements for solar noon on a winter's day are presented in Table 6 below.

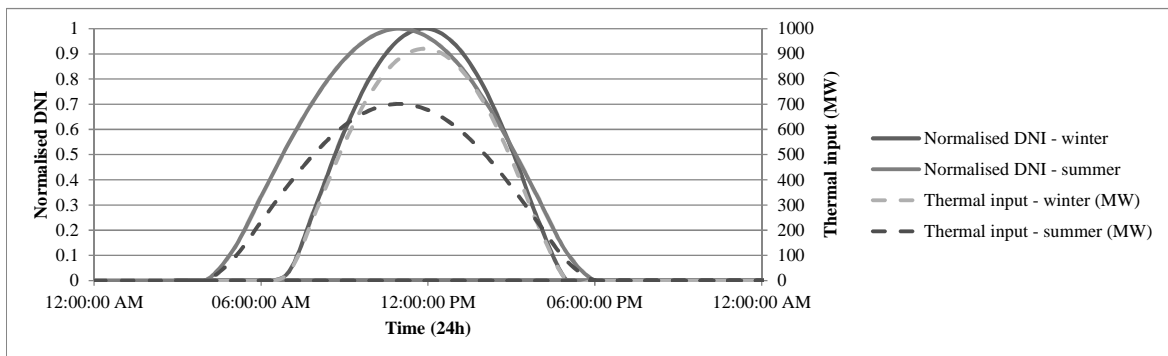


**Fig.7. - Normalised DNI and thermal input profiles for Uppington for summer and winter**

A heat transfer model is needed for the sizing of the heat transfer surfaces of both the receiver and the heat exchangers in the storage units. The fluid properties of eutectic NaK is used, as specified in the *Liquid Metals Engineering handbook* [4].

The heat transfer model that describes the NaK-AISi12 heat transfer system, and is depicted in Figure 8, is relatively simple compared to the steam system. Instead of solidified PCM accumulating around the heat transfer pipes, the AISi12 melts around the heat transfer pipe, and the radius of molten PCM will continue to increase.

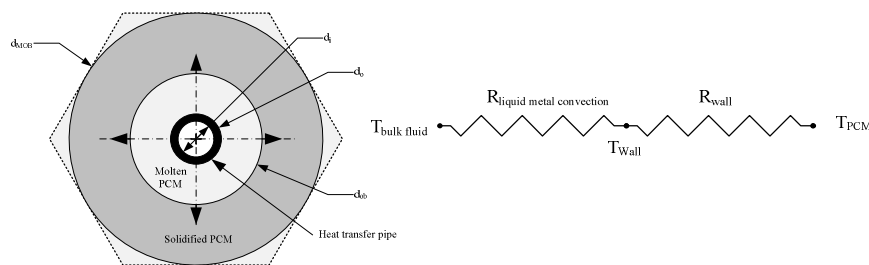


**Fig.8. - NaK heat transfer model**

The Nusselt number for the liquid metal convective heat transfer is calculated using the Seban-Shimazaki correlation [4]. This heat transfer model has been implemented in Flownex and the accuracy of the model has been improved by further discretisation of the heat transfer elements.

Using the heat transfer requirements presented in Table 6, it was possible to design the NaK heat exchangers. The design geometry is presented in Table 4 above, and a schematic of the model is shown in Figure 9 below

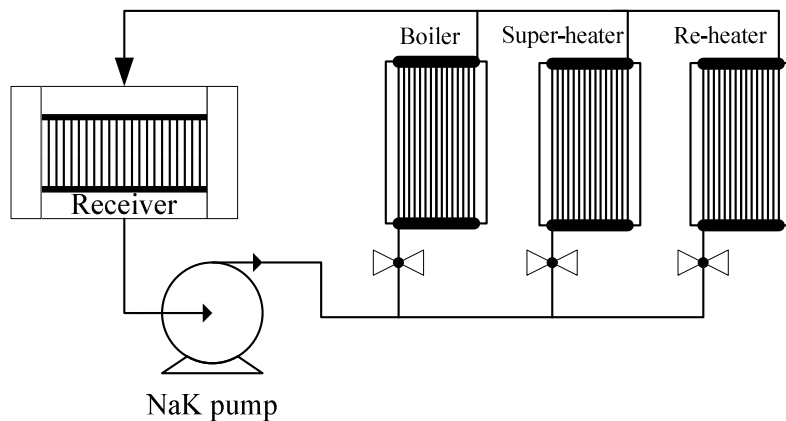


**Fig.9. - Primary cooling loop (NaK)**

	Unit	Boiler	Super-heater	Re-heater	Receiver
NaK flow rate	kg/s	3120	1317	562	5000
Heat transfer requirements	MW	511	269	139	920
Inlet temperature	°C	849	849	849	656
Outlet temperature	°C	678	634	584	849

**Table 6 - NaK heat transfer conditions at peak conditions (solar noon in winter)**

## 7. Conclusion

Metallic, latent heat thermal energy storage has the potential of providing thermal energy storage at temperatures as high as 946°C with storage densities as high as 757 kJ/kg (AlSi12, by comparison, has a melting point of 577°C and heat of fusion of 548.6J/g). This may significantly increase the thermal efficiency of a CSP plant and may substantially reduce the cost to build such a plant.

To investigate the feasibility and to aid in the design of a CSP plant using metallic phase-change materials, a Flownex model has been created. This model included a steam cycle, heat transfer models, a thermal energy storage model and a model of a primary heat transfer loop using NaK.

A simplified solar input model based on the Bird clear sky model was implemented; and will be replaced with a more advanced model incorporating the effects of a collector field, receiver performance and weather data. This model enables steady- and transient state modelling of the entire power cycle. Every aspect of the model can be changed during investigations; allowing for sensitivity analysis on the overall operational parameters of the power plant. The flexibility of the model allows the alteration of component models to suit the nature of the analysis. This model is based on a number of assumptions that are currently in a series of experiments for verification.

A power plant design has been proposed using the model, and the heat transfer surfaces and flow components have been sized. Although the proposed model is not optimized, the model enables the optimization of various components in more detailed studies. The will also enable a cost analysis of the system.

## References

- [1] J.P. Kotzé, T.W. von Backström & P.J. Erens., A Combined Latent Thermal Energy Storage and Steam Generator Concept Using Metallic Phase Change Materials and Metallic Heat Transfer Fluids for Concentrated Solar Power, SolarPACES 2011 – Granada.
- [2] M.M. Kenisarin, Renewable and Sustainable Energy Reviews, 14 (2010) 955-970.
- [3] J.P. Kotzé, T.W. von Backström, P.J. Erens, NaK as a primary heat transfer fluid in thermal solar power installations, SASEC 2012 – Stellenbosch.
- [4] O.J. Foust, (1972). Sodium-NaK engineering handbook, New York.
- [5] A. Bejan, Revue Générale de Thermique, 35 (1996), 418-419.
- [6] V. Gnielinski, Forschung im Ingenieurwesen, 41(1975), 8-16.
- [7] D. Steiner, J. Taborek, Heat Transfer Engineering, 13 (1992), 43-69.
- [8] Flownex theory manual, (2011).
- [9] J.C. Chen, Ind. Eng. Chem. Process Des. Dev., 5 (1966), 322-329.
- [10] R.E. Bird, R.L. Hulstrom, SERI Technical Report, (1991) 642-761.
- [11] F. Li, Y. Hu, R. Zhang, Advanced Materials Research, (2011), 239-242.